

Impact of three years of data from the Wilkinson Microwave Anisotropy Probe on cosmological models with dynamical dark energy

Michael Doran,^{*} Georg Robbers,[†] and Christof Wetterich[‡]

Institut für Theoretische Physik, Philosophenweg 16, 69120 Heidelberg, Germany

(Received 17 October 2006; published 10 January 2007)

The first three years of observation of the *Wilkinson Microwave Anisotropy Probe* (WMAP) have provided the most precise data on the anisotropies of the cosmic microwave background (CMB) to date. We investigate the impact of these results and their combination with data from other astrophysical probes on cosmological models with a dynamical dark energy component. By considering a wide range of such models, we find that the constraints on dynamical dark energy are significantly improved compared to the first year data.

DOI: [10.1103/PhysRevD.75.023003](https://doi.org/10.1103/PhysRevD.75.023003)

PACS numbers: 95.36.+x, 98.70.Vc, 98.80.Es

I. INTRODUCTION

Observations of type Ia supernovae (SNe Ia) [1,2], structure formation (LSS) [3,4] and the cosmic microwave background (CMB) [5–7] all agree on an accelerated expansion of our Universe. This rather unexpected phenomenon can be explained by modifying 4-D gravity [8,9] or adding a new component to the total energy momentum tensor. The simplest such component is a cosmological constant. It fits all current observations flawlessly and has a simple interpretation in terms of a vacuum energy. Yet, its observed value is 120 orders of magnitude off from the naive estimate $\Lambda \sim M_p^4$, where M_p is the reduced Planck mass. The coincidence between this minute dark energy contribution and the observed energy density of matter is rather puzzling. If not given by chance via some sort of anthropic principle, it necessitates a mechanism that explains this coincidence. An immediate possibility is a coupling [10–12] between (dark) matter and dark energy (though there might be problems due to quantum effects [13]).

Another solution is an attractor behavior [14–16] of dark energy that leads to an almost constant ratio between the fractional energy density $\Omega_d(z)$ of dark energy and the species otherwise dominating the expansion, i.e. photons and neutrinos during radiation domination and matter during matter domination. Coincidentally, such an attractor behavior corresponds to a scalar field with exponential potential that arises in string theories and when solving the cosmological constant problem from the point of view of dilatation symmetry [14]. The nonvanishing $\Omega_d(z)$ at higher redshifts alleviates the problem of explaining the coincidence of matter and dark energy today $\Omega_m^0 \approx \Omega_d^0$. Instead of fine tuning Λ to many orders of magnitude, the tuning needed is of the order of 10^{-3} . However, the tuning needed for such *early dark energy* cosmologies increases

the less dark energy there is at earlier times. A detection of early dark energy, on the other hand, would give crucial hints to fundamental laws of nature. The aim of this study therefore is to investigate the implications of the 3 yr data of WMAP on dynamical dark energy models in general and their respective fractions of early dark energy.

In view of the theoretical uncertainties many different techniques have been employed in the analysis of the dark energy, ranging from attempts to reconstruct the potential of a scalar field dark energy (e.g. Ref. [17]) to the principal component approach of Ref. [18]. We consider the redshift dependence of the fractional dark energy $\Omega_d(z)$ as a free function to be “measured” by observation. We investigate in this paper various parametrizations and an interpolated model. The possible coupling between dark energy and dark matter is neglected in this study.

II. OBSERVATIONAL TESTS

Dark Energy influences the expansion history of our Universe. In particular, the age t_0 , conformal horizons of today τ_0 and at last scattering τ_{ls} and the sound horizon r_s at last scattering are modified. The effects can be understood analytically [19–21] using an effective description in terms of weighted averages relevant for the epoch of last scattering

$$\Omega_d^e \equiv \tau_{ls}^{-1} \int_0^{\tau_{ls}} \Omega_d(\tau) d\tau \quad (1)$$

and structure formation

$$\bar{\Omega}_{sf} \equiv [\ln a_{tr} - \ln a_{eq}]^{-1} \int_{\ln a_{eq}}^{\ln a_{tr}} \Omega_d(a) d \ln a, \quad (2)$$

where $a_{tr} \approx 1/3$. The effect of dark energy on the CMB is twofold. Through the modified expansion history, it changes the acoustic scale l_A . In addition, it leads to a decay of the gravitational potential that is seen as an integrated Sachs-Wolfe contribution and a suppression of fluctuations on small scales [22]. The suppression of

^{*}Electronic address: M.Doran@thphys.uni-heidelberg.de

[†]Electronic address: G.Robbers@thphys.uni-heidelberg.de

[‡]Electronic address: C.Wetterich@thphys.uni-heidelberg.de

growth can be understood by looking at the equation of motion for cold dark matter perturbations inside the horizon, where the dark energy fluctuations are negligible [23]:

$$\ddot{\delta}_m + \frac{\dot{a}}{a} \dot{\delta}_m - \frac{3}{2} \left(\frac{\dot{a}}{a} \right)^2 \Omega_m \delta_m = 0. \quad (3)$$

Here the derivative is with respect to conformal time τ . In a matter Universe, $\Omega_m = 1$ and the solution is $\delta_m \propto a$. With dark energy present, $\Omega_m < 1$ and the growth of structure slows down according to the solution of (3) [23]

$$\delta_m \propto a^{\sqrt{25-24\Omega_d}-1}/4 \approx a^{1-3\Omega_d/5}. \quad (4)$$

This suppression starts as soon as a mode enters the horizon. As δ_m cannot grow during radiation domination, this leads to a red tilt of the CMB and matter power spectra up to the scale of the mode entering just at matter-radiation equality k_{equ} . All modes with $k > k_{\text{equ}}$ have been inside the horizon before equality and are suppressed by the same factor. Hence, early dark energy mimics to some extent a running spectral index with the important difference that the running stops at k_{equ} . All in all, the suppression leads to a smaller σ_8 compared to a Λ -CDM universe according to [19]

$$\frac{\sigma_8(Q)}{\sigma_8(\Lambda)} \approx (a_{\text{eq}})^{3\bar{\Omega}_{\text{sf}}/5} (1 - \Omega_\Lambda^0)^{-(1+\bar{w}^{-1})/5} \sqrt{\frac{\tau_0(Q)}{\tau_0(\Lambda)}}, \quad (5)$$

where τ is the conformal horizon today and \bar{w} is a suitably defined average equation of state of dark energy. As a rough rule of thumb, an increase of $\bar{\Omega}_{\text{sf}}$ by 10% leads to a decrease of σ_8 by 50%. In the following numerical analysis, we will not use constraints on the overall normalization of the power spectrum, i.e. we marginalize over the bias of 2dF and SDSS. As we will see, the data we use nevertheless constrains $\bar{\Omega}_{\text{sf}}$.

In contrast to linear growth, nonlinear structure formation is enhanced in early dark energy cosmologies. The density contrast δ_c corresponding to a collapsed structure is lower than in Λ -CDM [21]. As the abundance is exponentially sensitive to δ_c , the cluster abundance is considerably higher for a given σ_8 , as compared to Λ -CDM. In particular, the abundance of clusters at higher redshift drops more slowly than in Λ -CDM, which will soon be probed by gravitational lensing and Sunyaev-Zel'dovich surveys.

III. INVESTIGATED MODELS

Constraints on the values of cosmological parameters are always model dependent. For this analysis, we therefore select dark energy models with a large variety of different and in part opposite physical properties. This approach allows to identify the model dependencies of

the best fit ranges for the standard cosmological parameters, and their sensitivity to a change of the underlying dark energy behavior as compared to the Λ -CDM model. The first of these dark energy models is a leaping kinetic term model (“LKT”), where a change of the kinetic term of a scalar field at late times leads to acceleration [24]. In addition, we consider two models described by a parametrization of the evolution of the dark energy fraction $\Omega_d(a)$. In one of these models [25], Ω_d rather slowly relaxes from today’s Ω_d^0 to an asymptotic early-time value of Ω_\star and Ω_d can be written as $\Omega_d = \Omega_d(w_0, \Omega_\star)$. The other parametrization [26], which is a function of w_0 and Ω_d^e exhibits a faster variation of Ω_d and is characterized by a minimum amount of dark energy Ω_d^e throughout all cosmological epochs. This essentially fixes Ω_d to Ω_d^e from early times until redshifts of a few. We also include two models which parameterize the equation of state $w(a)$ of dark energy. The versatile parametrization of Bassett *et al.* [27], generalized by Corasaniti and Copeland in Ref. [28] (“C&C”), has four parameters for the equation of state, namely, its value today w_0 , its value during the matter dominated era w_m as well as the scale factor a_c^m and width Δ_m of the transition between these values, so that $w = w(w_0, w_m, a_c^m, \Delta_m)$. In addition, we consider the simple parametrization $w(a) = w_0 + w_1(1 - a)$ [29,30] frequently used in the literature. Finally, we analyze a model with Ω_d linearly interpolated in $\ln a$ between values at $z = 1, 3, 10, 100$ and $z = 1100$, leaving considerable freedom for the variation of $\Omega_d(a)$ at the cost of a rather large number of model parameters.

In addition to their respective dark energy parameters, all models depend on the standard cosmological parameters: the present matter energy fraction Ω_m and baryon energy fraction Ω_b , the Hubble parameter h , optical depth τ , scalar spectral index n_s and the initial scalar amplitude A_s , which we took into account using the observationally relevant combination $\ln(10^{10} A_s) - 2\tau$. We chose flat priors on all parameters.

The equation of state of the LKT and the $\Omega_d(w_0, \Omega_\star)$ -models was not allowed to cross the cosmological constant boundary of $w = -1$, and their fluctuations were treated like scalar field perturbations. The other models were allowed to cross $w = -1$. For these models, the speed of sound $c_s^2 = \delta p / \delta \rho$ was fixed at $c_s^2 = 1$, so that the perturbation equations for the pressure fluctuations remain well-defined even at the crossing. For the interpolated and the $\Omega(w_0, \Omega_d^e)$ models, this procedure was only adopted when the equation of state was close to the crossing, and the fluctuations were treated as scalar field perturbations everywhere else, so that these models had the usual scalar field perturbations during almost the entire evolution. This treatment is necessary because a single scalar field cannot traverse $w = -1$ [31–35].

These models were compared to two different sets of data. Set I are the WMAP 3-year data, and set II consists of WMAP [5], BOOMERANG’03 [36], VSA [37], CBI [6],

ACBAR [38] for the CMB plus 2DF [3] and SDSS [4] for LSS and SNe Ia data [1,2] combined. We omitted the baryon acoustic oscillation data [39], as it is currently not as sensitive as CMB and LSS in constraining early dark energy [40].

IV. RESULTS

The results are summarized in Fig. 1, which yields both the constraints on each of the standard parameters for all six of the models as well as their scatter. Also shown are

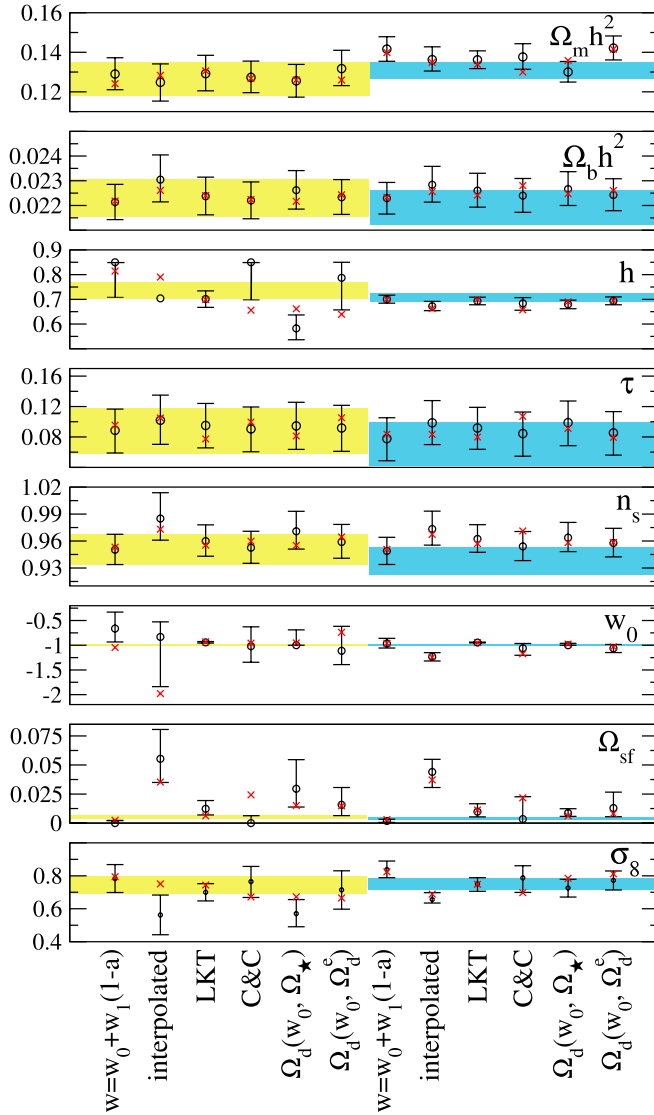


FIG. 1 (color online). Monte Carlo results for the cosmological parameters. The left-hand side shows the 1σ confidence intervals for the comparison of the models to the 3-year data of WMAP, the right-hand side corresponds to the results for the analysis with the combined set II. The shaded regions depict the 1σ intervals for the Λ -CDM analysis from WMAP for the WMAP data only and the “all” set, respectively. The crosses show the value of the respective parameter for the best fit model in the Monte Carlo chains.

the values for $\bar{\Omega}_{sf}$ and σ_8 . As a first result from the Monte Carlo analysis, we find that cosmological models with a dynamically evolving dark energy component fit the data as well as Λ -CDM, but not better. Secondly, the constraints on the standard cosmological parameters are well compatible with the results found by WMAP for a Λ -CDM cosmology, almost irrespective of the assumed behavior of the dark energy. Models that allow for a significant amount of dark energy at early times do have, however, a few significant features. Most prominently, they have a lower σ_8 from the linear analysis, as expected. In the light of the rather low scalar spectral index n_s found by WMAP, one might have suspected that dynamical dark energy models would allow for a scalar spectral index that would be closer to $n_s = 1$, which corresponds to a scale invariant spectrum of the initial fluctuations. However, all investigated dynamical dark energy models show a preference for $n_s < 1$, extending the result found by WMAP to a wider range of cosmological models.

The one sigma bounds on the dark energy fraction for the interpolated model are shown in Fig. 2. It is apparent from this plot that, while the preferred amount of dark energy in this model includes the values typical for Λ -CDM cosmologies, it also allows for much larger fractions of dark energy for redshifts $z = 3$ and higher. The evolution of the dark energy density $\sim \Omega_d h^2$ can be substantial and is not required to be monotonic in this model. This can lead to pronounced ISW contributions. With Ω_d as a free parameter at different z , the model can to some extent “manufacture” the shape of the TT -power spectrum at scales larger than the first peak, leading to a good fit to the WMAP-3 data. This, however, comes at the cost of

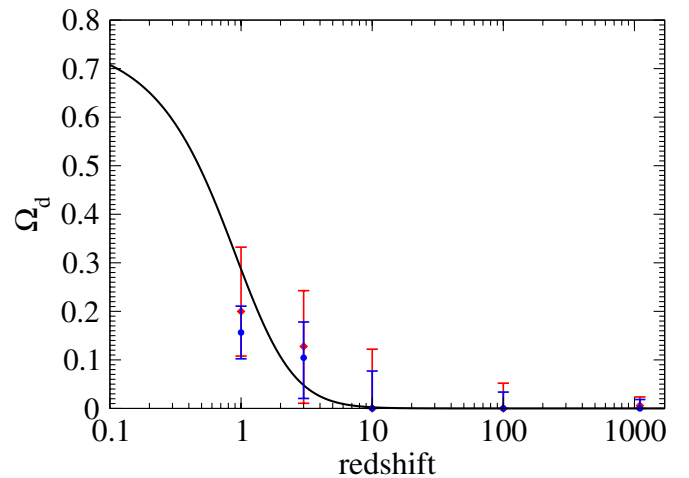


FIG. 2 (color online). One-sigma confidence intervals for the fraction of dark energy at different redshifts for the interpolated model. Red is the result obtained by comparing to the WMAP 3-year data, blue (lower) corresponds to the combined set II as described in the text. The black line shows the evolution of Ω_Λ for a Λ -CDM universe with the WMAP 3-year best fit values for the standard cosmological parameters.

severely suppressing σ_8 and is in conflict with the data of set II. Furthermore, with WMAP-3 alone, the Hubble parameter is considerably less constrained for this model. This is due to the fact that with $\Omega_d(z)$ for $z > 1$ given by the model's parameters independent of h , the acoustic scale l_A depends only very weakly on h . The relative independence of Ω_d in one redshift bin from its neighboring values also leads to the Monte Carlo algorithm finding a comparatively high number of well-fitting models with rather high $\bar{\Omega}_{sf}$. The interpolated models consequently have the highest values of $\bar{\Omega}_{sf}$, with the upper 2σ limit reaching $\bar{\Omega}_{sf} \lesssim 11\%$ for WMAP-3 alone and 6.5% from the combined set II.

The 2σ upper bounds of the other models for $\bar{\Omega}_{sf}$ from WMAP-3 alone vary from a very low 0.5% , caused by the choice of parametrization for the $w(a) = w_0 + w_1(1 - a)$ model, to $\sim 5\%$ for the $\Omega(w_0, \Omega_d^e)$ -model and $\sim 7\%$ for the model with $\Omega_d = \Omega_d(w_0, \Omega_*)$. This represents a decrease of about one to 2% compared to the first year data. For the combined set II, the upper bound decreases for all these models to less than about 3% , with the $\Omega(w_0, \Omega_d^e)$ -model yielding the highest value of $\bar{\Omega}_{sf} \lesssim 4\%$. We recall that already a few percent of $\bar{\Omega}_{sf}$ can have important effects on the abundance of nonlinear structure at high redshift [21].

V. CONCLUSIONS

The 3 year data of WMAP was used to estimate cosmological parameters for a wide range of dynamical dark energy models. We have shown that this new data in combination with large scale structure data constrain the average amount of dark energy during the time of structure formation to $\bar{\Omega}_{sf} \lesssim 4\%$ for a fair sample of dark energy models from the literature. We have also constructed a parametrization of $\Omega_d(a)$ which linearly interpolates between the dark energy fraction at several redshift bins. This allows for a considerably higher fraction of $\bar{\Omega}_{sf}$. The analysis also shows that the values of the standard cosmological parameters for the dynamical dark energy models are well compatible with the values found by WMAP for Λ -CDM. The effect of dynamical dark energy on σ_8 and on the formation of nonlinear structure offer promising routes for further constraints on the time evolution of dark energy or a possible falsification of the Λ -CDM model.

ACKNOWLEDGMENTS

We acknowledge the use of the Legacy Archive for Microwave Background Data Analysis (LAMBDA). Support for LAMBDA is provided by the NASA Office of Space Science.

-
- [1] P. Astier *et al.*, *Astron. Astrophys.* **447**, 31 (2006).
 - [2] A. G. Riess *et al.* (Supernova Search Team Collaboration), *Astrophys. J.* **607**, 665 (2004).
 - [3] W. J. Percival *et al.* (The 2dFGRS Collaboration), *Mon. Not. R. Astron. Soc.* **327**, 1297 (2001).
 - [4] M. Tegmark *et al.* (SDSS Collaboration), *Phys. Rev. D* **69**, 103501 (2004).
 - [5] D. N. Spergel *et al.*, *astro-ph/0603449*.
 - [6] A. C. S. Readhead *et al.*, *Astrophys. J.* **609**, 498 (2004).
 - [7] J. H. Goldstein *et al.*, *Astrophys. J.* **599**, 773 (2003).
 - [8] G. R. Dvali, G. Gabadadze, and M. Porrati, *Phys. Lett. B* **485**, 208 (2000).
 - [9] J. D. Bekenstein, *Phys. Rev. D* **70**, 083509 (2004); **71**, 069901(E) (2005).
 - [10] C. Wetterich, *Astron. Astrophys.* **301**, 321 (1995).
 - [11] L. Amendola, *Phys. Rev. D* **62**, 043511 (2000).
 - [12] L. Amendola, M. Quartin, S. Tsujikawa, and I. Waga, *Phys. Rev. D* **74**, 023525 (2006).
 - [13] M. Doran and J. Jaeckel, *Phys. Rev. D* **66**, 043519 (2002).
 - [14] C. Wetterich, *Nucl. Phys.* **B302**, 668 (1988).
 - [15] B. Ratra and P. J. Peebles, *Phys. Rev. D* **37**, 3406 (1988).
 - [16] R. R. Caldwell, R. Dave, and P. J. Steinhardt, *Phys. Rev. Lett.* **80**, 1582 (1998).
 - [17] M. Sahlen, A. R. Liddle, and D. Parkinson, *astro-ph/0610812*.
 - [18] D. Huterer and G. Starkman, *Phys. Rev. Lett.* **90**, 031301 (2003).
 - [19] M. Doran, M. J. Lilley, J. Schwindt, and C. Wetterich, *Astrophys. J.* **559**, 501 (2001).
 - [20] M. Doran, J. M. Schwindt, and C. Wetterich, *Phys. Rev. D* **64**, 123520 (2001).
 - [21] M. Bartelmann, M. Doran, and C. Wetterich, *astro-ph/0507257*.
 - [22] R. R. Caldwell, M. Doran, C. M. Mueller, G. Schaefer, and C. Wetterich, *Astrophys. J.* **591**, L75 (2003).
 - [23] P. G. Ferreira and M. Joyce, *Phys. Rev. D* **58**, 023503 (1998).
 - [24] A. Hebecker and C. Wetterich, *Phys. Lett. B* **497**, 281 (2001).
 - [25] C. Wetterich, *Phys. Lett. B* **594**, 17 (2004).
 - [26] M. Doran and G. Robbers, *J. Cosmol. Astropart. Phys.* **06** (2006) 026.
 - [27] B. A. Bassett, M. Kunz, J. Silk, and C. Ungarelli, *Mon. Not. R. Astron. Soc.* **336**, 1217 (2002).
 - [28] P. S. Corasaniti and E. J. Copeland, *Phys. Rev. D* **67**, 063521 (2003).
 - [29] M. Chevallier and D. Polarski, *Int. J. Mod. Phys. D* **10**, 213 (2001).
 - [30] E. V. Linder, *Phys. Rev. Lett.* **90**, 091301 (2003).
 - [31] A. Vikman, *Phys. Rev. D* **71**, 023515 (2005).
 - [32] W. Hu, *Phys. Rev. D* **71**, 047301 (2005).

- [33] G. Huey, astro-ph/0411102.
- [34] R.R. Caldwell and M. Doran, Phys. Rev. D **72**, 043527 (2005).
- [35] G. B. Zhao, J. Q. Xia, M. Li, B. Feng, and X. Zhang, Phys. Rev. D **72**, 123515 (2005).
- [36] C.J. MacTavish *et al.*, Astrophys. J. **647**, 799 (2006).
- [37] C. Dickinson *et al.*, Mon. Not. R. Astron. Soc. **353**, 732 (2004).
- [38] C.I. Kuo *et al.* (ACBAR collaboration), Astrophys. J. **600**, 32 (2004).
- [39] D.J. Eisenstein *et al.*, Astrophys. J. **633**, 560 (2005).
- [40] M. Doran, S. Stern, and E. Thommes, astro-ph/0609075.